

# Unconventional superfluidity of fermions in Bose-Fermi mixtures

O. Dutta<sup>1</sup> and M. Lewenstein<sup>1,2</sup>

<sup>1</sup> *ICFO-Institut de Ciències Fotòniques, Mediterranean Technology Park, 08860 Castelldefels (Barcelona), Spain, and*

<sup>2</sup> *ICREA-Institució Catalana de Recerca i Estudis Avançats, Lluís Companys 23, 08010 Barcelona, Spain.*

(Dated: April 26, 2018)

We examine two dimensional mixture of single-component fermions and dipolar bosons. We calculate the self-energies of the fermions in the normal state and the Cooper pair channel by including first order vertex correction to derive a modified Eliashberg equation. We predict appearance of superfluids with various non-standard pairing symmetries at experimentally feasible transition temperatures within the strong-coupling limit of the Eliashberg equation. Excitations in these superfluids are anyonic and follow non-Abelian statistics.

PACS numbers:

## I. INTRODUCTION

Experimental realization of fermionic superfluidity in a quantum degenerate ultracold gas [1] started a renewed interest in the field. Attraction between fermionic particles favours pairing of fermions resulting in superfluidity of the system. The paired fermions, known as Cooper pairs, can have different kinds of internal symmetries. The common ones found in nature have  $s$ -wave and  $d$ -wave internal structure and conserve parity and time reversal symmetry. In superfluid  $^3\text{He}$ , the so-called  $A$  and  $A_1$  phases are characterized by Cooper pairs with nonzero magnetic orbital momenta. Also, there was a theoretical prediction of higher order  $f$ -wave pairing in  $^3\text{He}$  [2, 3]. Cooper pairs with chiral  $p_x + ip_y$ -wave internal structure are believed to be responsible for the observed superfluidity of electrons in Strontium Ruthenate [4]. This kind of pairing breaks the time-reversal symmetry. Spinless chiral  $p$ -wave superfluid state has formal resemblance to the ‘‘Pfaffian’’ state proposed in relation to the fractional quantum Hall state with filling factor  $5/2$  [5–7]. When confined in a two dimensional geometry, excitations in the chiral  $p$ -wave superfluid become so called non-Abelian anyons. Anyons are particles living in a two dimensional plane that under exchange do not behave neither as bosons nor as fermions. For non-Abelian anyons, exchange of two such particles depends on the order of the exchange [8–10]. Apart from fundamental interest in the existence of such particles, non-Abelian anyons find remarkable applications in the field of quantum information for quantum memories and fault-tolerant quantum computation [11].

Recently it has been shown that quasi-particles in vortex excitations of chiral two-dimensional  $p$ -wave spinless superfluids obey non-Abelian statistics [12, 13]. Using  $p$ -wave Feshbach resonances in fermionic ultracold atoms, such superfluids can be realized in principle, but this procedure is very difficult because of non-elastic loss processes [14]. Another proposal for  $p$ -wave superfluid with dipolar fermions has been recently formulated in Ref [15] with transition temperature in the order of  $.1\epsilon_f$ , where  $\epsilon_f$  is the Fermi energy. Bose-Fermi mixtures are another candidate for creating superfluidity in fermions via boson

mediated interactions [16] and have formal resemblance to phonon mediated superconductivity in metals. It was found, however, when the bosons and single-component fermions are completely mixed, increasing the boson-fermion interaction strength, or fermionic density may induce dynamical instability of the condensate resulting in phase separation between the mixture [16–19]. Near phase separation, inclusion of the dressing of phonons is predicted to increase the transition temperature. In Ref. [20], the authors found that close to Feshbach resonances, a Bose condensate of dimers can induce a strong pairing in the  $p$ -wave channel.

In the present paper, we discuss another way to generate high temperature superfluids in a Bose-Fermi mixture. We study the property of superfluidity in Bose-Fermi mixtures, where bosons are interacting via long-ranged dipolar interactions. We show that the transition temperature for  $p$ -wave superfluidity can become comparable to the Fermi energy. More importantly, we find that other more exotic Cooper pairs with  $f$ - and  $h$ -wave internal symmetries are possible in certain range of Fermi energies without bosons and fermions separating. In addition, we study the excitations in chiral states of the odd-wave superfluids and point out their non-Abelian anyonic nature. Experimentally, an available bosonic species, where prominent dipolar interaction can be achieved using Feshbach resonance is  $\text{Cr}^{52}$  [23, 24]. Another route towards achieving ultracold dipolar gas is to experimentally realize quantum degenerate heteronuclear molecules [25], which have permanent electric moment. Thus, in the near future a quantum degenerate mixture of dipolar bosons and fermions will be achievable experimentally.

In Section II we review the properties of a dipolar Bose condensate in a pancake trap. We discuss specially the excitation spectrum of such condensates. Then in Section III we study the boson-fermion interaction and the many-body effect of fermions on dressing the excitation spectrum of the condensate. In Section IV, we discuss the interaction between the fermions mediated by bosons in different angular momentum channel. By integrating out the bosonic mode, we show that the absolute value of the interaction between fermions in the  $p$ ,  $h$ ,  $f$ -wave angular momentum channel are comparable depending on

the Fermi energy. In Section V, we go beyond Migdal's limit and include first order vertex corrections to study fermion self-energy in normal state as well as the mass renormalization function in the high temperature limit. In doing so, we include the full effect of retardation and strong momentum dependence of the bosonic excitation spectrum and bosonic propagator. We find that vertex correction reduces the mass renormalization function. In Section VI we calculate the self-energy in Cooper-pair channel for  $p$ ,  $f$ ,  $h$ -wave order parameters including the vertex correction and cross-interaction for temperature  $T > T_c$ . By deriving a vertex-corrected strong-coupling Eliashberg equation, we solve for transition temperatures in different angular momentum channels. In Section VII, we present a brief discussion regarding the possible occurrence of non-Abelian Majorana fermions for broken time-reversal  $p$ ,  $f$ , and  $h$ -wave superfluids. We solve the Bogoliubov-deGennes equation for the  $p$ ,  $f$ , and  $h$ -wave superfluids in the limit of large distance to find the Majorana bound states.

## II. DIPOLAR BOSE-EINSTEIN CONDENSATE

Our system consists of dipolar bosons mixed with single component fermions, confined in a quasi-two dimensional geometry by a harmonic potential in the  $z$  direction with the condition  $m_b\omega_b^2 = m_f\omega_f^2$  where  $m_b$  and  $m_f$  is the mass of bosons and fermions respectively and  $\omega_b, \omega_f$  is the trapping frequency. First, we assume that the bosons are polarized along the  $z$  direction. The dipolar interaction reads  $V_{dd} = \frac{4\pi g_{dd}}{3}(3k_z^2/k^2 - 1)$  in momentum space, where  $g_{dd}$  is the dipole-dipole interaction strength. For atoms  $g_{dd} = \mu_0\mu_m^2/4\pi$ , and for dipolar molecules  $g_{dd} = \mu_e^2/4\pi\epsilon_0$ , where  $\mu_m$  and  $\mu_e$  are the magnetic moment of the atoms and the electric dipole moment of the molecules, respectively. We assume that the  $z$  dependence of bosonic density is given by a Thomas-Fermi profile,

$$n_b(x, y, z) = \frac{3n_b}{4R_z} \left(1 - \frac{z^2}{R_z^2}\right),$$

where the Thomas-Fermi radius  $R_z$  is determined variationally. After integrating over  $z$  dependence of the density profile of bosons, the total interaction takes the form  $V_{\text{eff}} = \frac{8\pi g_{dd}}{5R_z} \mathcal{V}(\tilde{k}_\perp)$  where

$$\begin{aligned} \mathcal{V}(\tilde{k}_\perp) &= \frac{3g}{8\pi g_{dd}} - \frac{1}{2} \\ &+ \frac{15[2\tilde{k}_\perp^3 - 3\tilde{k}_\perp^2 - 3(1 + \tilde{k}_\perp)^2 \exp(-2\tilde{k}_\perp) + 3]}{8\tilde{k}_\perp^5}, \end{aligned} \quad (1)$$

$\tilde{k}_\perp = k_\perp R_z$  and  $g$  is the contact interaction between the bosons.  $\mathcal{V}(k_\perp)$  is repulsive for small momentum and can be attractive in the high momentum limit depending on the contact interaction. Subsequently, we write

the Hamiltonian of the dipolar bosons in the condensed phase,  $H_b = \sum_{k_\perp} \Omega_0(k_\perp) \beta_{k_\perp}^\dagger \beta_{k_\perp}$ , where  $\beta_{k_\perp}^\dagger$  and  $\beta_{k_\perp}$  are Bogoliubov operators. The excitation frequency  $\Omega_0(k_\perp)$  is given in the units of trap frequency,

$$\Omega_0^2(k_\perp \ell_0) = \frac{[k_\perp \ell_0]^4}{4} + g_{3d} \frac{\ell_0}{R_z} \mathcal{V}\left(k_\perp \ell_0 \frac{R_z}{\ell_0}\right) [k_\perp \ell_0]^2, \quad (2)$$

where  $\ell_0 = \sqrt{\hbar/m_b\omega_b}$ . We define a dimensionless dipolar interaction strength  $g_{3d} = 8\pi m_b g_{dd} n_b \ell_0 / 5\hbar^2$  which will be used later, where  $\ell_0$  is the ground state oscillator length. Also the phonon propagator  $D_0(i\omega_s, k_\perp)$  in this regime is given by

$$D_0(i\omega_s, k_\perp) = -\frac{\Omega_0(k_\perp)}{\omega_s^2 + \Omega_0^2(k_\perp)}, \quad (3)$$

where bosonic Matsubara frequency  $\omega_s = 2s$  where  $s$  is an integer. By minimizing the mean field energy of the Bose condensate within Thomas-Fermi regime we find that

$$R_z/\ell_0 = \left(2.5g_{3d} \left[1 + \frac{3}{16\pi g_{dd}}\right]\right)^{1/3}.$$

For  $\frac{3g}{4\pi g_{dd}} > 1$ , the excitation spectrum of the condensate, denoted by  $\Omega(k_\perp)$ , can be divided into two parts: i)  $\sim k_\perp$ , phonon spectrum for small momenta and ii)  $\sim k_\perp^2$ , free-particle like spectrum for higher momenta [26]. For  $\frac{3g}{4\pi g_{dd}} < 1$  and  $g_{3d}$  greater than a critical value,  $\Omega(k_\perp)$  has a minimum at momentum  $\tilde{k}_0$  [29], where  $\tilde{k}_0$  is in intermediate momentum regime. Following Landau, the excitations around the minimum are called "rotons". With increasing  $g_{3d}$  the excitation energy at  $\tilde{k}_0$  decreases and eventually vanishes for a critical particle density. When the particle density exceeds that critical value, the excitation energy becomes imaginary at finite momentum and the condensate becomes unstable. The use of Thomas-Fermi density profile is justified in this region as the chemical potential necessary to reach roton instability exceeds  $\hbar\omega_z$ .

## III. BOSON-FERMION INTERACTION AND DRESSED EXCITATION

In this section, first we discuss the condensate-fermion interaction Hamiltonian and dynamical stability of the condensate. We find the dressed propagator for the Bogoliubov quasi-particles in presence of fermionic particle hole excitation within second-order perturbation theory. We then discuss the appearance of roton instability in the dressed excitation spectrum of the condensate.

Kinetic energy for the single component non-interacting fermions, is characterized by the Hamiltonian  $H_f = \sum_{k_\perp} [\xi(k_\perp) - \epsilon_f] c_{k_\perp}^\dagger c_{k_\perp}$ , where  $c_{k_\perp}^\dagger$  and  $c_{k_\perp}$  are fermionic creation and destruction operator.  $\xi(k_\perp) =$

$\vec{k}^2/2m_f - \epsilon_f$  is the dispersion energy of the fermions and  $\epsilon_f$  is the Fermi energy. The density profile of fermions along the  $z$  direction is approximated by a normalized Gaussian with width  $\ell_f = \sqrt{\hbar/m_f\omega_f}$ . The fermions are interacting with the bosons via short ranged contact interaction of strength  $g_{\text{bf}}$ . After integrating over the  $z$  coordinate, the boson-fermion interaction Hamiltonian reads

$$H_{\text{bf}} = \frac{3g_{\text{bf}}\alpha}{4\sqrt{\pi}R_z} \sum_{\vec{k}_\perp, \vec{q}_\perp} c_{\vec{k}_\perp}^\dagger c_{\vec{k}_\perp} b_{\vec{q}_\perp}^\dagger b_{\vec{q}_\perp}, \quad (4)$$

where  $b_{\vec{q}_\perp}, b_{\vec{q}_\perp}^\dagger$  are bosonic creation and annihilation operator, and  $\alpha = \frac{\ell_f}{R_z} \exp\left(-\frac{R_z^2}{\ell_f^2}\right) - \frac{\sqrt{\pi}}{2} \left(\frac{\ell_f^2}{R_z^2} - 2\right) \text{erf}\left(\frac{R_z}{\ell_f}\right)$ , with  $\text{erf}(\cdot)$  being the error function. Next, we concentrate our attention on the interaction between the fermions and the Bogoliubov quasi-particles. The fluctuations in fermionic density couple to the density fluctuations present in the Bose condensate. Due to the momentum dependence of the bosonic excitations, the condensate-fermion interaction becomes function of momentum. Including the fluctuations in the Bose condensate in the  $x-y$  plane, the condensate-fermion interaction Hamiltonian can be written as

$$H_{\text{bf}} = \frac{3g_{\text{bf}}}{4\sqrt{\pi}R_z} \alpha \sum_{\vec{k}_\perp, \vec{q}_\perp} \gamma(\vec{k}_\perp) c_{\vec{k}_\perp}^\dagger c_{\vec{q}_\perp - \vec{k}_\perp} [b_{\vec{k}_\perp} + b_{-\vec{k}_\perp}^\dagger], \quad (5)$$

where the momentum dependent coupling constant is given by  $\gamma(\vec{k}_\perp) = \sqrt{2n_b\epsilon_b(\vec{k}_\perp)/\Omega_0(\vec{k}_\perp)}$ . Due to the inter-

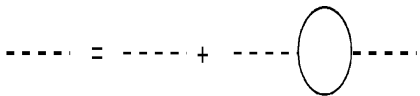


FIG. 1: Schematic diagram of phonon propagator including the polarizing effect of the fermions. The thick dash-dotted line corresponds to the dressed phonon propagator  $D(i\omega_s, k_\perp)$ , while the thin dash-dotted line corresponds to non-interacting phonon propagator  $D_0(i\omega_s, k_\perp)$ . The solid line corresponds to free fermion propagator.

action between Bogoliubov quasi-particles and fermions, as shown in Fig. 1, the bosonic excitations are dressed by the fermions resulting in dressing of bare condensate excitation spectrum in Eq. (2). This can be derived within second order perturbation theory as shown in Fig. 1. Subsequently the new phonon propagator is given by

$$D(i\omega_s, k_\perp) = -\frac{\Omega_0(k_\perp)}{\omega_s^2 + \Omega^2(k_\perp)}, \quad (6)$$

where the dressed excitation spectrum  $\Omega(k_\perp \ell_0)$  for the dressed Bogoliubov quasi-particles is expressed by

$$\Omega(k_\perp) = \Omega_0(k_\perp) \sqrt{1 - \frac{|\gamma(k_\perp)|^2 N_0}{\Omega_0(k_\perp)} h(\omega, k_\perp)}, \quad (7)$$

where the two dimensional Lindhard function

$$h(\omega, k_\perp) = 1 - |\omega| \frac{\theta(|\omega| - v_f k_\perp)}{\sqrt{\omega^2 - v_f^2 k_\perp^2}},$$

and  $\omega$  is the transfer of energy. As we are interested in Cooper instability of the fermions which happens for momenta close to Fermi momentum, the transfer of energy is of the order of  $\omega \ll \epsilon_f$ . In this limit the Lindhard function  $h(\omega, k_\perp) = 1$ . For future use, we define an effective interaction strength between the bosons and fermions,

$$\mathcal{G}_{\text{bf}} = \frac{45g_{\text{bf}}^2 N_0}{128\pi g_{\text{dd}} \ell_0} \alpha^2.$$

In order to determine dynamical stability of the uniform condensate, we study the properties of the dressed spectrum of Bogoliubov quasi-particles in the parameter regime of  $\frac{3g}{4\pi g_{\text{dd}}} > 1$ , where the bare spectrum has no roton minimum. From Eq. (7), due to the attractive effect of Bose-Fermi interaction, we notice that roton minimum in the excitation spectrum  $\Omega(k_\perp)$  can develop for certain critical interaction strength  $g_{3d}$  and  $\mathcal{G}_{\text{bf}}$ . Consequently, the uniform condensate will become unstable as the excitation spectrum becomes imaginary at a finite momentum. But, as long as the roton gap remains positive, the uniform state of the bosons will be stable or metastable [28]. In Fig. 2, we have plotted the dressed excitation spectrum for different values of Bose-Fermi interaction  $\mathcal{G}_{\text{bf}}$ . With no boson-fermion interaction, as  $\frac{3g}{4\pi g_{\text{dd}}} > 1$ , the excitation spectrum has the usual phonon regime for low momenta and free particle regime for higher momenta. For a critical  $\mathcal{G}_{\text{bf}}$ , i.e.  $\mathcal{G}_{\text{bf}} \approx .5$  in Fig. 2, in the region of intermediate momenta, the excitation spec-

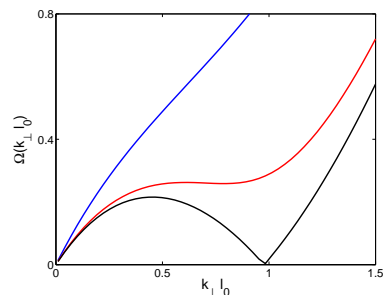


FIG. 2: The dressed excitation spectrum  $\Omega(k_\perp)$  as a function of  $k_\perp$ . For various values of the Bose-Fermi interaction  $\mathcal{G}_{\text{bf}} = 0$  (blue line),  $.51$  (red line),  $.57$  (black line). The fixed parameters are  $m_f = 53$ ,  $\frac{3g}{4\pi g_{\text{dd}}} = .6$ , and  $g_{3d} = 2.5$

trum have roton-maxon character. With further increase of  $\mathcal{G}_{\text{bf}}$ , the roton gap goes to zero and the excitation spectrum becomes imaginary at a finite momentum. Subsequently the bosons undergo a phase transition to a state with periodic density modulation, which finally collapses. This periodic density wave state can be stabilized for repulsive contact interaction obeying  $3g/8\pi g_{\text{dd}} \approx \mathcal{G}_{\text{bf}} \frac{\ell_0}{R_z}$

[28]. The appearance of roton minimum in dressed excitation spectrum in this case is entirely due to the many-body effect of the fermions on Bogoliubov quasi-particles. Another point we like to stress is that, the roton instability is always reached before the phonon instability pointing towards phase separation [16].

#### IV. EFFECTIVE INTERACTION BETWEEN FERMIONS

In this section we find the interaction between the fermions mediated by the Bogoliubov quasi-particles in the limit of  $T = 0$ . We then obtain the interaction strength in different angular momentum channel, which varies as a function of *dimensionality* parameter, defined as  $\eta = \epsilon_f/\hbar\omega_f$ .

Integrating out the bosonic degree of freedom in Eq. (5), and inclusion of the effect of dressed excitation spectrum, results in effective interaction between the fermions [30],

$$V_{\text{ph}}(\vec{q}_{\perp}, i\omega_s) = \frac{9g_{\text{bf}}^2\alpha^2}{16\pi R_z^2} \frac{n_b q_{\perp}^2/m_b}{\omega^2 - \Omega^2(\vec{q}_{\perp})}, \quad (8)$$

where  $q_{\perp}^2 = 2k_f^2(1 - \cos\phi)$ , is the momentum exchange between the interacting particles along the Fermi surface. At  $T = 0$ , assuming momentum transfer occur around Fermi momentum  $k_f$ , we can expand Eq. (8) as  $V_{\text{ph}}(\vec{k}_{\perp}, 0) = -\sum_{L=\dots,-1,0,1,\dots} \lambda_L(0,0)e^{iL\phi}$ , and the dimensionless effective interaction between the fermions in angular momentum channel  $L$  is given by

$$\lambda_L(0,0) = \mathcal{G}_{\text{bf}} \int_0^{2\pi} \frac{\exp[iL\phi]d\phi/2\pi}{\frac{\eta R_z^2}{g_{3d}\ell_f^2}(1 - \cos\phi) + \frac{R_z}{\ell_0}\mathcal{V}(\sqrt{\frac{R_z}{\ell_f}}\eta(1 - \cos\phi))}. \quad (9)$$

As we are considering single component fermions, pairing will occur in the odd angular momentum channels.

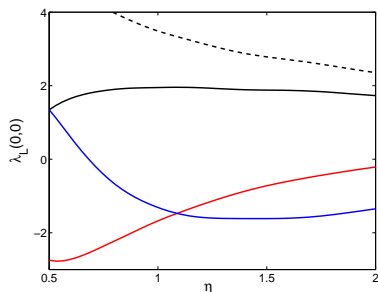


FIG. 3: Figure of effective fermion-fermion interaction strength  $\lambda_L(0,0)$  in the angular momentum channels  $L = 0$ (dashed line),  $L = 1$ (black line),  $L = 3$ (red line),  $L = 5$ (blue line) as a function of the fermion dimensionality parameter  $\eta$ . We fixed  $mf/mb = 53/52$ ,  $g_{3d} = 4$ ,  $3g/8\pi g_{\text{ad}} = 0.6$ , and  $\mathcal{G}_{\text{bf}} = 0.5$ .

Next, we look into the variation of  $\lambda_L(0,0)$  as a function of  $\eta$ . For concreteness, we assume a  $^{52}\text{Cr}$ - $^{53}\text{Cr}$  mixture. The interaction strengths from Eq. (9) in various angular momentum channels have been plotted in Fig. 3. We find that with changing dimensionality, the strengths in different angular momentum channel varies. Additionally,  $|\lambda_1(0,0)| \sim |\lambda_3(0,0)| \sim |\lambda_5(0,0)|$ , and depending on the dimensionality they can be positive or negative.

#### V. FERMIONIC SELF-ENERGY INCLUDING VERTEX CORRECTION

In this section, we consider the fermion self-energy in the normal state due to the interaction between the fermions and dressed Bogoliubov quasi-particles. In doing so, we explicitly take into account the momentum dependence as well as the retardation of the phonon propagator. More importantly, we also go beyond Migdal's adiabatic limit and take into account the effect of vertex correction. This kind of non-adiabatic correction is introduced to electron-phonon system in metals in Refs [31–33] in the limit of  $T \rightarrow 0$ . Our main result is that as temperature gets lower, the vertex-corrected mass renormalization function  $Z(T)$  also gets smaller.

The unperturbed Green's function for the fermions is given by  $G_0(\vec{k}_{\perp}, i\omega_n) = 1/(i\omega_n - \xi(\vec{k}_{\perp}))$ , where the Matsubara frequency  $\omega_n = (2n+1)\pi T$ ,  $n$  being integer. The

$$\Sigma_n = \text{---} \text{---} \text{---} + \text{---} \text{---} \text{---} \quad (9)$$

FIG. 4: Figure of fermion self-energy in normal state including the first order vertex correction. The solid line denotes the fermion propagator while the thick dashed line denotes the dressed phonon propagator of Eq. (6)

normal self-energy  $\Sigma_n(\vec{k}_{\perp})$ , including the first order vertex correction, as shown in Fig. 4, is given by

$$\Sigma_n(\vec{k}_{\perp}, i\omega_n) = \Sigma_n^1(\vec{k}_{\perp}, i\omega_n) + \Sigma_n^v(\vec{k}_{\perp}, i\omega_n), \quad (10)$$

where  $\Sigma_n^1(\vec{k}_{\perp}, i\omega_n)$  comes from the first diagram in Fig. 4 and  $\Sigma_n^v(\vec{k}_{\perp}, i\omega_n)$  arises from the second diagram which denotes the vertex correction. Also,

$$\begin{aligned}\Sigma_n^1(\vec{k}_\perp, i\omega_n) &= -T \sum_{m, \vec{q}_\perp} |\gamma(\vec{k}_\perp - \vec{q}_\perp)|^2 D(\omega_m - \omega_n, \vec{k}_\perp - \vec{q}_\perp) G_0(i\omega_m, \vec{q}_\perp), \\ \Sigma_n^v(\vec{k}_\perp, i\omega_n) &= T^2 \sum_{m, l, \vec{q}_\perp, \vec{p}_\perp} |\gamma(\vec{k}_\perp - \vec{q}_\perp)|^2 |\gamma(\vec{k}_\perp - \vec{p}_\perp)|^2 D(\omega_l - \omega_n, \vec{k}_\perp - \vec{p}_\perp) D(\omega_m - \omega_n, \vec{k}_\perp - \vec{q}_\perp) \quad (11) \\ &\times G_0(i\omega_m, \vec{q}_\perp) G_0(i\omega_l, \vec{p}_\perp) G_0(i(\omega_l - \omega_n + \omega_m), \vec{p}_\perp - \vec{k}_\perp + \vec{q}_\perp),\end{aligned}$$

(12)

By taking the average over Fermi energy ( $|\vec{k}_\perp| \approx |\vec{q}_\perp| \approx k_f$ ), and denoting  $\xi(\vec{k}_\perp) = \hbar^2 k_\perp^2 / 2m - \epsilon_f = x$ ,  $\xi(\vec{p}_\perp) = \hbar^2 k_\perp^2 / 2m - \epsilon_f = x'$ , and  $\xi(\vec{p}_\perp - \vec{k}_\perp + \vec{q}_\perp) - \mu = x' + 2\epsilon_f \alpha$ , where

$$\alpha = 1 - \cos(\phi') + \cos(\theta) - \cos(\gamma) \quad (13)$$

and the angles  $(\vec{k}_\perp, \vec{q}_\perp) = \phi'$ ,  $(\vec{k}_\perp, \vec{p}_\perp) = \theta$ ,  $\gamma = \phi' - \theta$ . Using Euler-Mclaurin summation formula, we can transform the sum over  $l$  in Eq. (11) to integral as,

$$\begin{aligned}P(x', m, T, \phi', \theta) &= - \sum_l D(\omega_l - \omega_n, \vec{k}_\perp - \vec{p}_\perp) \quad (14) \\ &\times G(i\omega_m, \vec{q}_\perp) G(i\omega_l, \vec{p}_\perp) G(i(\omega_l - \omega_n + \omega_m), \vec{p}_\perp - \vec{k}_\perp + \vec{q}_\perp) \\ &= \int_{-\infty}^{+\infty} \frac{d\omega}{2\pi} \frac{\Omega^2}{\omega^2 + \Omega^2} \frac{1}{i\omega - x' + i\pi T} \frac{1}{(\omega + 2m\pi T) - x' - \alpha + i\pi T} \\ &= \frac{i\Omega}{2(2m\pi T - i\alpha)} \left[ \frac{\theta(x')}{\Omega + x' - i\pi T} - \frac{\theta(-x')}{\Omega - x' + i\pi T} \right. \\ &\quad \left. - \frac{\theta(x' + \alpha)}{\Omega - 2im\pi T + x' - i\pi T + \alpha} + \frac{\theta(-x' - \alpha)}{\Omega + 2im\pi T - x' + i\pi T - \alpha} \right], \quad (15)\end{aligned}$$

here  $\theta(\cdot)$  is the Step function. We can rewrite  $\Sigma_n(i\omega_n)$  as

$$\Sigma_n(i\omega_n) = \chi(i\omega_n) + i\omega_n[1 - Z(i\omega_n)], \quad (16)$$

where  $\chi(i\omega_n)$  is the real part of  $\Sigma_n(i\omega_n)$  and  $Z(i\omega_n)$  is known as the mass renormalization function.  $\chi(\pi T)$  shifts the bare fermion dispersion energy  $\xi(\vec{k}_\perp)$ . As we are considering strong-coupling superfluidity, we only consider the term corresponds to  $n = 0$  [41]. Then the mass renormalization function  $Z(\pi T)$  and  $\chi(\pi T)$  in the

conventional Eliashberg form is given by,

$$Z(\pi T) = 1 + \lambda_Z(T), \quad (17)$$

$$\chi(\pi T) = \sum_m \text{sign}(\omega_m) \text{Im}[P_v(m, T)], \quad (18)$$

with an effective coupling constant

$$\lambda_Z(T) = \lambda_0(0, 0) - P_v(T), \quad (19)$$

and  $P_v(T) = \sum_m \text{sign}(\omega_m) \text{Re}[P_v(m, T)]$ , where

$$\begin{aligned}\lambda_L(s, T) &= - \int_0^{2\pi} |\gamma(\phi)|^2 D(\omega_s, \phi) \cos L\phi d\phi / 2\pi, \\ P_v(m, T) &= \int_{-\epsilon_f}^{\epsilon_f} dx' \int_{-\pi}^{\pi} \frac{d\phi'}{2\pi} d\theta |\gamma(\phi')|^2 |\gamma(\theta)|^2 P(x', m, T, \phi', \theta), \quad (20)\end{aligned}$$

and  $\text{Re}[f]$ ,  $\text{Im}[f]$  denotes the real and imaginary part

of the function  $f$ . In Fig. 5 we plot  $P_v(T)$  as a func-

tion of temperature for various values of dimensionality  $\eta$ . From the expression of  $\lambda_L(s, T)$  in Eq. (20), we notice that  $\lambda_L(0, 0)$  is always positive as shown in Fig. 3.  $P_v(T)/\lambda_0(0, 0)$  is the expansion parameter for the perturbative scheme. The correction  $P_v(T)$  is always found to be positive, which reduces the coupling strength  $\lambda_Z(T)$ . With decreasing temperature,  $P_v(T)/\lambda_0(0, 0)$  increases before saturating. This saturation value increases with decreasing dimensionality as seen in Fig. 5. For smaller  $\eta$ ,  $P_v(T)\lambda_0(0, 0)$  becomes higher than one for lower temperature, invalidating any perturbative calculation in that low temperature region.

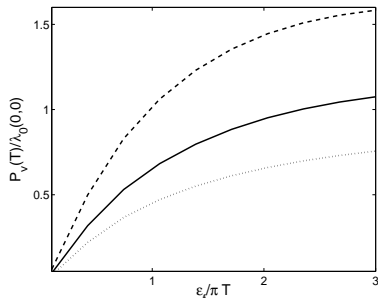


FIG. 5: Plot of the vertex correction in  $P_v$  as a function of  $\frac{\epsilon_f}{\pi T}$  for different values of the dimensionality parameter  $\eta = 1.5$  (the dotted line),  $\eta = 1$  (the solid line),  $\eta = .6$  (the dashed line). We fixed  $m_f/m_b = 53/52$ ,  $\frac{3g}{4\pi g_{dd}} = .6$ ,  $\mathcal{G} = .5$ , and  $g_{3d} = 3.8$ .

Next, we calculate the real part of the fermion self energy  $\chi(\pi T)$ . Figure 6 shows a such generic case for

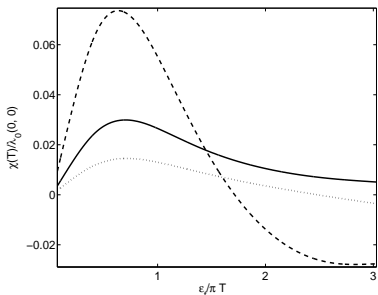


FIG. 6: Figure of  $\chi(T)$  as a function of  $\frac{\epsilon_f}{\pi T}$  for different values of the dimensionality parameter  $\eta = 1.5$  (the dotted line),  $\eta = 1$  (the solid line),  $\eta = .6$  (the dashed line). We fixed  $m_f/m_b = 53/52$ ,  $\frac{3g}{4\pi g_{dd}} = .6$ ,  $\mathcal{G} = .5$ , and  $g_{3d} = 3.8$ .

the same parameters as Fig. 5. We find that  $\chi(T) \ll \lambda_0(0, 0)$  even in the temperature region with high  $P_v(T)$ . Henceforth, we can neglect the effect of energy shift of the fermions due to the smallness of  $\chi(T)$ .

## VI. SELF-ENERGY IN COOPER-PAIR CHANNEL AND TRANSITION TEMPERATURE

In this section we look at the fermionic self-energy in the Cooper-pair channel,  $\Sigma_s(\vec{k}_\perp, i\omega_n)$  as represented diagrammatically in Fig. 7, close to transition temperature  $T_c$ . Then we find transition temperature within strong-coupling limit considering the terms  $n = 0, -1$  [34]. The main results of this section are : *i*) Depending on the angular momentum channel, the vertex-corrected interaction strength can increase as a function of dimensionality and temperature. *ii*) The solution of modified Eliashberg equation supports  $T_c \sim .1\epsilon_f$  in the strong-coupling limit for  $p-$ ,  $f-$ , and  $h-$  wave order parameters.

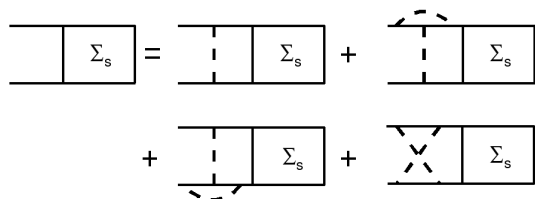


FIG. 7: Schematic diagram of fermion self-energy in the Cooper-pair channel including the first order vertex correction. The solid line denotes the fermion propagator while the thick dashed line denotes the dressed phonon propagator of Eq. (6). The first diagram denotes the direct interaction, while the second and third diagram denote the first order vertex corrections, and the third diagram denotes the cross-term.

For  $T > T_c$ , the fermion self-energy in the Cooper-pair channel,  $\Sigma_s(\vec{k}_\perp)$ , is given by

$$\Sigma_s(\vec{k}_\perp, i\omega_n) = \Sigma_s^1(\vec{k}_\perp, i\omega_n) + \Sigma_s^v(\vec{k}_\perp, i\omega_n) + \Sigma_s^c(\vec{k}_\perp, i\omega_n), \quad (21)$$

where  $\Sigma_s^1(\vec{k}_\perp, i\omega_n)$  comes from the first diagram in Fig. 7, the second and third diagram gives equal contribution and denoted by  $\Sigma_s^v(\vec{k}_\perp, i\omega_n)$  while the last diagram denoting cross interaction is given by  $\Sigma_s^c(\vec{k}_\perp, i\omega_n)$ , and

$$\Sigma_s^1(\vec{k}_\perp, i\omega_n) = -T \sum_{m, \vec{q}_\perp} |\gamma(\vec{k}_\perp - \vec{q}_\perp)|^2 D(\omega_m - \omega_n, \vec{k}_\perp - \vec{q}_\perp) G(i\omega_m, \vec{q}_\perp) G(-i\omega_m, -\vec{q}_\perp) \Sigma_s(\vec{q}_\perp, i\omega_m), \quad (22)$$

$$\begin{aligned} \Sigma_s^v(\vec{k}_\perp, i\omega_n) &= 2T^2 \sum_{m, l, \vec{q}_\perp, \vec{p}_\perp} |\gamma(\vec{k}_\perp - \vec{q}_\perp)|^2 |\gamma(\vec{k}_\perp - \vec{p}_\perp)|^2 D(\omega_m - \omega_n, \vec{k}_\perp - \vec{q}_\perp) D(\omega_n - \omega_l, \vec{k}_\perp - \vec{q}_\perp) \\ &\times G(i\omega_l, \vec{p}_\perp) G(i(\omega_l - \omega_n + \omega_m), \vec{p}_\perp - \vec{k}_\perp + \vec{q}_\perp) G(i\omega_m, \vec{q}_\perp) G(-i\omega_m, -\vec{q}_\perp) \Sigma_s(\vec{q}_\perp, i\omega_m), \end{aligned} \quad (23)$$

$$\begin{aligned} \Sigma_s^c(\vec{k}_\perp, i\omega_n) &= T^2 \sum_{m,l,\vec{q}_\perp,p_\perp} |\gamma(\vec{k}_\perp - \vec{p}_\perp)|^2 |\gamma(\vec{q}_\perp - \vec{p}_\perp)|^2 D(\omega_n - \omega_l, \vec{k}_\perp - \vec{p}_\perp) D(\omega_m - \omega_l, \vec{q}_\perp - \vec{p}_\perp) \\ &\times G(i\omega_l, \vec{p}_\perp) G(i(\omega_l - \omega_n - \omega_m), \vec{p}_\perp - \vec{k}_\perp - \vec{q}_\perp) G(i\omega_m, \vec{q}_\perp) G(-i\omega_m, -\vec{q}_\perp) \Sigma_s(\vec{q}_\perp, i\omega_m), \end{aligned} \quad (24)$$

We take the average over Fermi energy ( $|\vec{k}_\perp| \approx |\vec{q}_\perp| \approx k_f$ ), and denote  $\xi(\vec{p}_\perp - \vec{k}_\perp - \vec{q}_\perp) - \mu = x' + 2\epsilon_f\beta$ , where

$$\beta = 1 + \cos(\phi') - \cos(\theta) - \cos(\gamma).$$

We define the superfluid order parameter in the usual way,  $\Delta(i\omega_n) = \Sigma_s(i\omega_n)/Z(i\omega_n)$ . Due to single-component nature of the fermions in the mixture, the order parameter can be expanded in odd partial wave  $\Delta(i\omega_n, \phi) = \sum_{L=\dots,-1,1,\dots} \Delta_L(i\omega_n) \exp[iL\phi]$ . In the strong coupling limit we are interested in the terms  $n = 0$  and  $n = -1$  [41]. Assuming the order parameter to be even function of frequency,  $\Delta(\pi T) = \Delta(-\pi T)$ , we get

from Eq. (21), (22),

$$\Delta_L(\pi T) Z(\pi T) = \lambda_L^\Delta(0, T) \Delta_L(\pi T) + \lambda_L^\Delta(-1, T) \Delta_L(-\pi T), \quad (25)$$

where

$$\lambda_L^\Delta(m, T) = \lambda_L(m, T) - 2P_v(m, T) - P_c(m, T), \quad (26)$$

$\lambda_L(m, T)$  originate from  $\Sigma_s^1(i\omega_n)$ , whereas  $P_v(m, T)$  comes from vertex corrected self-energy  $\Sigma_s^v(i\omega_n)$ .  $P_c(m, T)$  results from the contribution the cross-term  $\Sigma_s^c(i\omega_n)$ ,

$$\begin{aligned} P_c(m, T) &= 2T \text{Im} \left[ \sum_{l,\phi',\theta} |\gamma(\theta)|^2 |\gamma(\theta - \phi')|^2 D(l, \theta - \phi') D(m - l, \phi') \right. \\ &\times \left. \left[ \tan^{-1} \left[ \frac{\mu}{(2l+1)\pi T} \right] - \tan^{-1} \left[ \frac{\mu}{i\beta + (2l-2m-1)\pi T} \right] \right] \frac{1}{\beta + 2i(m+1)\pi T} \right]. \end{aligned} \quad (27)$$

Eq. (25) is similar to the Eliashberg equation [41] in the strong coupling limit with additional vertex-corrected interaction strengths. Apart from the dependance on temperature, the effective interaction strength in the angular momentum channel  $L$ ,  $\lambda_L^\Delta(T)$ , is also a function of dimensionality  $\eta$  and the boson-fermion mass ratio  $m_f/m_b$ . As noticed in Eq. (20),  $P_v(0, T)$  is positive, thus reducing the effective interaction strength in the Cooper-pair channel. But the correction arising from the cross term  $P_c(m, T)$  can be negative or positive, as shown in Fig. 8. Also the sign of  $P_c(m, T)$  depends on the particular angular momentum channel under consideration. But in general, for smaller  $\eta$ ,  $P_c(m, T)$  becomes positive, in turn reducing the interaction strength,  $\lambda_L^\Delta(m, T)$ , in the Cooper-pair channel. But higher value of  $\eta$  changes  $P_c(m, T)$  to negative, which enhances  $\lambda_L^\Delta(m, T)$ . We also find out that with increasing fermionic mass,  $P_c(m, T)$  becomes negative for lower values of  $\eta$ , thus enhancing the interaction strengths in the various angular momentum channel. The reason behind this is that  $P_c(m, T)$  depends on the ratio between the position of the roton minimum  $k_0$  and Fermi momentum  $k_0/2k_f$ . With high fermionic mass,  $k_f$  increases, resulting in lower ratio  $k_0/2k_f$ . This in turn makes the cross term more negative. From this we infer

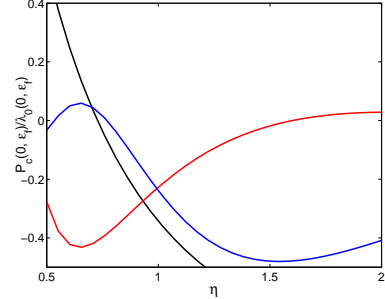


FIG. 8: Plot of cross-term interaction  $P_c(0, \epsilon_f)$  as a function of  $\eta$  for  $m_f/m_b = 53/52$ ,  $\pi T = \mu$ ,  $g_{3d} = 4.0$ ,  $G_{bf} = 0.5$  and  $\frac{3g}{4\pi g_{3d}} = 0.6$ . The black, red and blue lines correspond to  $p$ ,  $f$ , and  $h$ -wave angular momentum channel respectively.

that it is better to use fermions with higher mass to get a higher interaction strength  $\lambda_L^\Delta(m, T)$ .

Next we look into the dependance of  $\lambda_L^\Delta(0, T)$  on dimensionality  $\eta$ . First we fix  $\pi T = \epsilon_f$  and plot for various value of  $\eta$  in Fig. 9. We see that the magnitude of  $\lambda_L^\Delta(\epsilon_f)$  in different angular momentum channel changes as  $\eta$  varies. Also different angular momentum channel be-

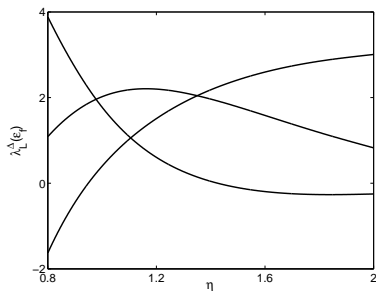


FIG. 9: Figure of effective interaction  $\lambda_L^\Delta(\pi T = \epsilon_f)$  as a function of  $\eta$  for  $m_f/m_b = 53/52$ ,  $\pi T = \epsilon_f$ ,  $g_{3d} = 4.0$ ,  $\mathcal{G}_{bf} = .5$  and  $\frac{3g}{4\pi g_{3d}} = .6$ . The black, red and blue lines correspond to  $\lambda_1^\Delta(T)$ ,  $\lambda_3^\Delta(T)$ ,  $\lambda_5^\Delta(T)$  respectively.

comes dominant depending on the dimensionality. This qualitatively resembles the situation in section 3, where without the vertex correction, we find that different interactions becomes dominant for different dimensionality.

Next we find the transition temperature for fermionic superfluidity within perturbative scheme as long as  $T_c < T^*$  where  $T^*$  is the temperature for which the perturbative scheme becomes invalid. In the situation of more than one solution of Eq. (25), we have taken the transition temperature to be the one corresponding to the highest temperature. In the case of Eq. (25) having no solution for  $T_c$ , vertex-corrected strong coupling superfluidity is not possible and to find the transition temperature we need to consider the full Eliashberg equation [41] for all values of  $n$ . This regime is not considered in this paper as we are only interested in the high temperature limit of the transition temperature. In Fig. 10 (a) and (b) we plot the solution of the Eqs. (17), (25). In the case of obtaining multiple solutions for transition temperature corresponding to different angular momentum channel, we considered the channel with maximum transition temperature to be the solution. In general we find that with lowering dimensionality, the nature of the superfluidity changes from  $p$ , to  $h$  to  $f$ -wave. Also we obtained transition temperature  $T_c$  in the order of  $.1\epsilon_f$  or more in each angular momentum channel. By comparing Fig. 10 (a) and (b) we notice that, for higher fermion mass, we find that much lower value of  $\eta$  can be attainable without the perturbation becoming invalid than for a lower fermionic mass.

## VII. CHIRALITY AND NON-ABELIAN ANYONS

In this section we briefly discuss the properties of quasi-particle excitations inside a vortex for different internal symmetries of the order parameter. By solving Bugoliubov-DeGennes equation in the limit of large distance from the core of the vortex, we show that the zero-energy solutions in the chiral  $p$ -,  $f$ -,  $h$ - wave states

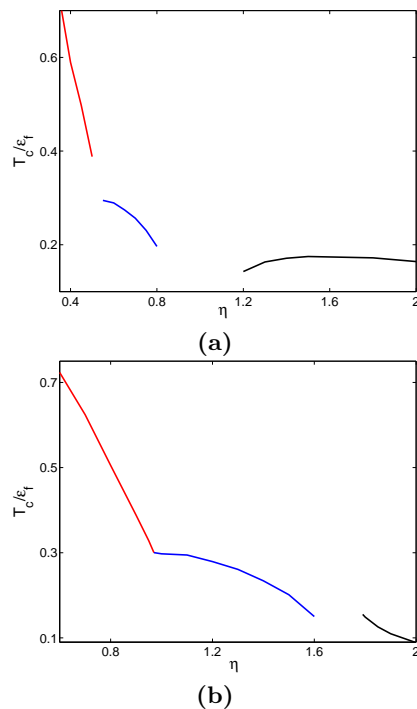


FIG. 10: Critical temperature  $T_c$ , in the units of Fermi energy  $\epsilon_f$ , as a function of  $\eta$ . The black, red and blue lines correspond to transition temperature of  $p$ -wave,  $h$ -wave, and  $f$ -wave order parameters respectively with parameters . a) For parameters  $m_f/m_b = 1.7$ , and dipole strength  $g_{3d} = 2.5$ . b) For parameters  $m_f/m_b = 53/52$ , and dipole strength  $g_{3d} = 4.0$ .

are bounded and non-Abelian in nature. By considering the superfluid gap equation at low temperature, the gap is maximum when the order parameter breaks time reversal symmetry. From now on we assume that the order parameters are denoted by  $\Delta_L = \Delta_0(\vec{r}) \left[ \frac{k}{k_f} \right]^L e^{iL\theta}$  where  $k_x = k \cos \theta$ ,  $k_y = k \sin \theta$  and  $\Delta_0(\vec{r})$  is the center of mass amplitude of the Cooper pairs, with  $\vec{r}$  being the center of mass coordinate of the pair. For vortex state  $\Delta_0(\vec{r})$  can be approximated as: i)  $\Delta_0(\vec{r}) = 0$ ,  $r < \xi$  and ii)  $\Delta_0(\vec{r}) = \Delta_0 \exp(i\phi)$ ,  $r \geq \xi$ , where  $r = \sqrt{x^2 + y^2}$ ,  $\tan \phi = y/x$ .  $\xi$  is the size of the core of the vortex. The vortex state of the  $p$ -wave superfluids always has a zero-energy bound quasi-particle state [6, 38, 39]. Now we discuss the asymptotic solutions for the zero-energy bound state for  $f$ - and  $h$ -wave order parameters. The quasi-particle states in a single vortex can be found in the limit of large distance from the vortex core by solving the Bugoliubov-DeGennes equation,

$$\begin{aligned} H_0 u_L + (-i)^L \frac{\Delta_0}{k_f^L} e^{i\phi/2} \left[ e^{-i\phi} \left( \frac{\partial}{\partial r} - \frac{i}{r} \frac{\partial}{\partial \phi} \right) \right]^L e^{i\phi/2} v_L \\ = E u_L \\ -H_0 v_L + (i)^L \frac{\Delta_0}{k_f^L} e^{-i\phi/2} \left[ e^{i\phi} \left( \frac{\partial}{\partial r} + \frac{i}{r} \frac{\partial}{\partial \phi} \right) \right]^L e^{-i\phi/2} u_L \end{aligned}$$

$$= Ev_L, \quad (28)$$

where  $E$  is the energy of the quasi-particles with amplitudes  $u_L, v_L$ . We particularly look for zero energy solutions with bounded  $u_L, v_L$  with the property  $u_L = v_L^*$  [38]. For  $r \rightarrow \infty$ , we can neglect the terms scaled as  $r^{-1}$  in Eq. (28). Then the solution of Eq. (28) with different orbital symmetries read,

$$\begin{bmatrix} u_1 \\ u_3 \\ u_5 \end{bmatrix} \sim \begin{bmatrix} \exp\left(-\frac{m_f \Delta_0}{k_f} r\right) \\ \exp\left(-\frac{k_f^3}{6m_f \Delta_0} r\right) e^{2i\phi} \\ \exp\left(-\left[\frac{k_f^5}{2m_f \Delta_0}\right]^{1/3} r\right) e^{4i\phi} \end{bmatrix}. \quad (29)$$

The zero-energy solution for each odd-wave parameter corresponds to different angular momentum channel of the quasi-particles inside a vortex core. These results can also be carried out by applying the ‘‘index theorem’’ [40]. For temperature smaller than the energy gap  $\Delta_0^2/\epsilon_f$ , only the zero energy mode is occupied. The quasi-particle operator in that situation is written as  $\gamma_L = \int d^2r (u_L(r)c^\dagger(r) + v_L(r)c(r))$ , which acts as Majorana fermion [6, 12, 38].  $\gamma_L$  obeys non-Abelian statistics and can be used for quantum computing [13]. In order to perform quantum computational tasks, existence of several well separated vortices is necessary. We can assume in the weak coupling limit,  $\Delta_0 = \beta\epsilon_f$ , where  $\beta$  is a constant usually less than one. Then substituting  $\Delta_0$  in Eq. (29), we get  $u_1 \propto \exp(-\beta k_f r/2)$ ,  $u_3 \propto \exp(-k_f r/3\beta)$ ,  $u_5 \propto \exp(-k_f r/\beta^{1/3})$ . For  $r \gg \xi$ , for

smaller  $\beta$ ,  $u_5$  has smaller tail than  $u_3$  and  $u_1$ . Thus non-overlapped states can be achieved more easily in superfluids in  $L = 5$  and  $L = 3$  channel than for p-wave channel.

## VIII. CONCLUSION

Summarizing, we studied boson-induced superfluidity of fermions in a mixture of dipolar bosons and single-component fermions. A system is proposed where conventional pairing mechanism gives rise to different exotic internal structures of the Cooper pairs with strong interaction in respective angular momentum channels. We find that vertex-corrections play an important role for superfluidity in this mixture and results in high value of transition temperatures. We like to stress that the high transition temperatures are a result of the inclusion of vertex correction and cross interaction within the Cooper-pair channel. Importantly, we find that by decreasing  $\eta$ , we can generate exotic superfluids with  $p$ ,  $f$  and  $h$ -wave internal structure. Excitations in these types of superfluids breaks time-reversal symmetry and supports quasi-particles with non-Abelian statistics.

## IX. ACKNOWLEDGEMENT

This work is financially supported by the Spanish MEC QOIT (Consolider Ingenio 2010) projects, TOQATA (FIS2008-00784), MEC/ESF project FERMIX (FIS2007-29996-E), EU IP grant AQUITE, ERC advanced grant QUAGATUA, and Humboldt Foundation.

- 
- [1] M. W. Zwierlein et al., *Science* **311**, 492 (2006).  
[2] G. Barton, and M. A. Moore, *J. Phys. C: Proc. Phys. Soc., London* **8**, 970 (1975)  
[3] N. D. Mermin, *Phys. Rev. B* **13**, 112 (1976).  
[4] Y. Maeno, T.M. Rice, and M. Sigrist, *Physics Today* **54**, 42 (2001).  
[5] R. L. Willett, et. al., *Phys. Rev. Lett.* **59**, 1776 (1987).  
[6] C. Nayak, S. H. Simon, A. Stern, M. Freedman, and S. Das Sarma, *Rev. Mod. Phys.* **80**, 1083 (2008).  
[7] N. Read, *Phys. Rev. B* **79**, 045308 (2009).  
[8] F. Wilczek, *Phys. Rev. Lett.* **48**, 1144 (1982).  
[9] F. Wilczek, *Phys. Rev. Lett.* **49**, 957 (1982).  
[10] F. Wilczek, *Fractional Statistics and Anyon Superconductivity*, World Scientific, Singapore, (1990).  
[11] A. Y. Kitaev, *Ann. Phys.* **303**, 2, (2003).  
[12] D. A. Ivanov, *Phys. Rev. Lett.* **86**, 268 (2001).  
[13] S. Tewari, S. Das Sarma, C. Nayak, C. Zhang, and P. Zoller, *Phys. Rev. Lett.* **98**, 010506 (2007).  
[14] J. Levinsón, N. R. Cooper, and V. Gurarie, *Phys. Rev. A* **78**, 063616 (2008).  
[15] N. R. Cooper, G. V. Shlyapnikov, arXiv: 0907.3080.  
[16] D. V. Efremov, and L. Viverit, *Phys. Rev. B* **65**, 134519 (2002).  
[17] J. Mur-Petit, A. Polls, M. Baldo, and H.-J. Schulze, *Phys. Rev. A* **69**, 023606 (2004).  
[18] K. Yang, *Phys. Rev. B* **77**, 085115 (2008).  
[19] K. Suzuki, T. Miyakawa, T. Suzuki, *Phys. Rev. A* **77**, 043629 (2008).  
[20] A. Bulgac, S. Yoon, *Phys. Rev. A* **79**, 053625 (2009).  
[21] Tin-Lun Ho and Roberto B. Diener, *Phys. Rev. Lett.* **94**, 090402 (2005).  
[22] T. Enss, W. Zwerger, *Eur. Phys. Jour. B* **68**, 383 (2009).  
[23] T. Lahaye, et al., *Nature* **448**, 672 (2007).  
[24] T. Koch, et al., *Nature Physics* **4**, 218 (2008).  
[25] S. Ospelkaus, K. K. Ni, M. H. G. de Miranda, B. Neyenhuis, D. Wang, S. Kotochigova, P. S. Julienne, D. S. Jin, J. Ye, arXiv:0811.4618.  
[26] L. Pitaevskii and S. Stringari, *Bose-Einstein condensation*, Clarendon Press, Oxford, (2003).  
[27] We determine the Thomas-Fermi radius  $R_z$  by minimizing the mean-field energy (with respect to  $R_z$ ) of the bosons interacting via  $V_{\text{eff}}(k_\perp)$ .  
[28] O. Dutta, R. Kanamoto, and P. Meystre, *Phys. Rev. A* **78**, 043608 (2008).  
[29] L. Santos, G. V. Shlyapnikov, and M. Lewenstein, *Phys. Rev. Lett.* **90**, 250403 (2003).  
[30] Daw-Wei Wang, *Phys. Rev. Lett.* **96**, 140404 (2006).  
[31] C. Grimaldi, L. Pietronero, and S. Strassler, *Phys. Rev.*

- Lett. **75**, 1158 (1995).
- [32] L. Pietronero, S. Strassler, and C. Grimaldi, Phys. Rev. B **52**, 10516 (1995).
- [33] C. Grimaldi, L. Pietronero, and S. Strassler, Phys. Rev. B **52**, 10530 (1995).
- [34] E. Cappelluti and G. A. Ummaryino, Phys. Rev. B **76**, 104522 (2007).
- [35] L. Viverit, C. J. Pethick, and H. Smith, Phys. Rev. A **61**, 053605 (2000).
- [36] Private communication with L. Santos.
- [37] J. P. Carbotte, Rev. Mod. Phys. **62**, 1027 (1990).
- [38] V. Gurarie and L. Radzihovsky, Phys. Rev. B **75**, 212509 (2007).
- [39] G. E. Volovik, The universe in a Helium Droplet, Clarendon Press, Oxford (2003).
- [40] S. Tewari, S. Das Sarma and Dung-Hai Lee, Phys. Rev. Lett. **99**, 037001 (2007).
- [41] G. D. Mahan, Many-Particle Physics, 3rd Edition, Kluwer Academic/Plenum Publishers, New York, (2000).